

van der Waals interactions mediating the cohesion of fullerenes on graphene

M. Švec,^{1,*} P. Merino,² Y. J. Dappe,^{3,4} C. González,¹ E. Abad,^{5,6} P. Jelínek,¹ and J. A. Martín-Gago^{2,7}

¹*Institute of Physics, Academy of Sciences of the Czech Republic, Cukrovarnická 10, CZ-16200 Prague, Czech Republic*

²*Centro de Astrobiología INTA-CSIC, Carretera de Ajalvir, km. 4, ES-28850 Madrid, Spain*

³*CEA, IRAMIS, SPCSI, F-91191 Gif sur Yvette, FRANCE*

⁴*Service de Physique de l'Etat Condensé, DSM/IRAMIS/SPEC, CEA Saclay URA CNRS 2464, F-91191 Gif-Sur-Yvette Cedex, France*

⁵*Departamento de Física Teórica de la Materia Condensada, Universidad Autónoma de Madrid, ES-28049 Madrid, Spain*

⁶*Computational Biochemistry Group, Institute of Theoretical Chemistry, University of Stuttgart, Pfaffenwaldring 55, D-70569 Stuttgart, Germany*

⁷*Instituto de Ciencia de Materiales de Madrid (CSIC), c/Sor Juana Inés de la Cruz, ES-28049 Madrid, Spain*

(Received 22 May 2012; revised manuscript received 4 September 2012; published 24 September 2012)

Fullerenes on single-layer epitaxial graphene are a model system to study very faint interactions at a molecular level. By a variable temperature scanning tunneling microscope we have been able to study ordered fullerene layers at 40 K, exclusively bound by van der Waals interactions. The experimentally determined adsorption geometry of the molecules is computationally confirmed only if van der Waals interactions are included in the calculation formalism. The relative orientation of fullerenes in their close-packed arrangement is found to be the crucial factor for determining the total energy. Observation of collective movements of fullerene islands points out the weak coupling to the substrate and the important role of the van der Waals cohesion forces within.

DOI: [10.1103/PhysRevB.86.121407](https://doi.org/10.1103/PhysRevB.86.121407)

PACS number(s): 81.05.ub, 81.05.ue, 36.40.Sx, 37.10.Mn

Mechanical stability, friction, or adhesion are among the physical properties that strongly depend on van der Waals (vdW) interactions. This is also true for the nanoscale. The nucleation and growth of molecular surface structures involve dynamic processes such as diffusion, molecular rotations, or conformational changes, which rely also on vdW intermolecular interactions.^{1,2} Moreover, self-assembly and adsorption studies focus on determining the preferred adsorption site and configuration, the adsorbate-adsorbate interaction, and the distance between the adsorbate and substrate (e.g., Ref. 3). There is an increasing interest in the role of vdW interactions of organic molecules on graphite and other surfaces.^{4,5}

Generally, long-distance forces as vdW are not described by the most widely used functionals of the density-functional theory (DFT). Thus, in many of the works performed until now they are simply not included. However, when planar systems of carbon-based materials are in question, they require a different approach to the interplay between intermolecular (lateral) and adsorbate-substrate (vertical) interactions in determining the properties of ordered molecular structures. To evidence the important role of the vdW interactions in adsorption processes we have chosen a system of a very weakly interacting substrate and adsorbate, single-layer graphene (SLG)⁶ and fullerenes (C₆₀).⁷ The fact that both materials consist exclusively of carbon atoms arranged in an atomically thin planar mesh without H or any other atoms inside the atomic structure that could lead to long-range H-bond interactions makes this system a good prototype for a demonstration of the effect of these forces at a molecular level.

Thus, we consider the C₆₀ on SLG grown on 6H-SiC(0001)^{8–10} as a model system to test the strength of the vdW forces and mutual interactions that occur between neutral inert nanostructures. C₆₀ adsorbed on surfaces generally tend to form hexagonal close-packed arrangements¹¹ in order to optimize their lateral interactions. In very recent studies of C₆₀ molecules deposited on SLG epitaxially grown on metal,^{12,13} it

has been shown that the interaction between the molecules and the substrate, and consequently the molecular arrangement, is ruled by the moiré unit cell. The C₆₀ coming to the surface are trapped in potential wells of the moiré valleys where the substrate SLG is more reactive, thus forming pinning centers for the other molecules that arrange in between. In contrast to these studies, we found a much weaker interaction of the C₆₀ with the SLG grown on 6H-SiC(0001), which lead us to a workbench to discuss the origin of the bonding mechanism in weakly interacting systems. Very recently a study of a very similar system appeared,¹⁴ which characterizes the basic behavior of the C₆₀ on a graphene layer at 6H-SiC(0001) near to one monolayer coverage and studies its electronic properties based on scanning tunneling spectroscopy.

We employed a variable temperature scanning tunneling microscope (VT-STM) and DFT-vdW calculations^{15–17} to prove that this system is solely governed by vdW forces. We determined the adsorption geometry of the molecules and we observed their collective motion. We also show that including vdW contribution in the calculations is necessary in order to fully describe theoretically the interaction between the *sp*² systems.

STM images of submonolayer coverage of C₆₀ molecules deposited at room temperature (RT) onto a 6H-SiC(0001) substrate partly covered with SLG show slightly disordered close-packed hexagonal planar islands of C₆₀ exclusively on the SiC buffer layer which has a quasi-6 × 6 periodicity (hereafter referred to as 6 × 6).⁹ That is, neither islands nor single molecules were spotted on the areas covered by SLG, because adsorbed C₆₀ diffuse out of the SLG regions.¹⁸ On the contrary, when we evaporate C₆₀ on the sample kept at a low temperature of 40 K (LT), STM images show the formation of C₆₀ epitaxial structures on SLG in the form of well-ordered planar islands with a configuration that seems to have a twofold symmetry. Figures 1(a) and 1(b) show the STM topography of islands on both types of surfaces and adsorbed

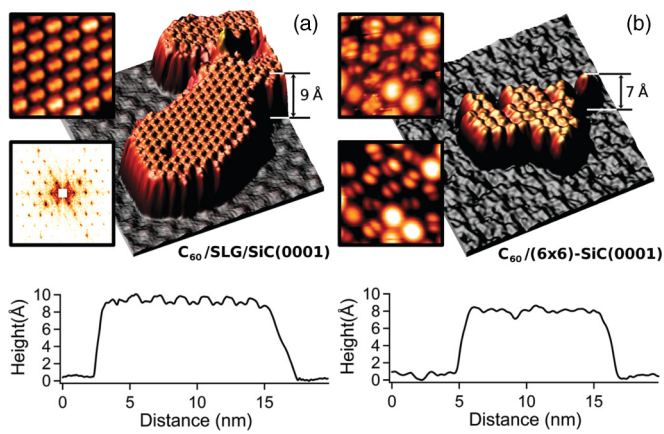


FIG. 1. (Color online) Three-dimensional (3D) representation of $20 \times 20 \text{ nm}^2$ empty states STM topography on C_{60} islands and their corresponding profiles: (a) SLG taken at 600 mV, 100 pA, with a $5 \times 5 \text{ nm}^2$ detail and FFT power spectrum of the entire area, showing a clear 4×4 pattern of the close-packed arrangement of the molecules on SLG. (b) (6×6) -SiC(0001) recorded at 1000 mV, 100 pA, and $5 \times 5 \text{ nm}^2$ insets showing two different types of submolecular resolution. Both images were obtained at 40 K.

molecules in detail, the latter imaged at two different levels of resolution.

At first glance the properties of the C_{60} islands on 6×6 [Fig. 1(b)] are very similar to the ones reported before at RT.^{19,20} The molecules inside the island are present in various orientations, i.e., different molecular orbitals (MO) are exposed to the probe during scanning. Their corrugation is 0.45 Å rms and the base apparent height is $7.2(\pm 0.5) \text{ Å}$. On larger scales, two quasiperiodic arrangements could be found corresponding to a pair of twin domains appearing at $\pm 20^\circ$ (with 1° error) with respect to 6×6 .

On the other hand, the C_{60} islands on SLG in Fig. 1(a) show lower corrugation (0.28 Å rms), a considerably denser packing, and an almost perfect order. According to the FFT power spectrum of the STM image in the inset of Fig. 1(a), the C_{60} molecules arrange in a 4×4 commensurate superstructure with respect to the SLG lattice. As a rule, the islands are hexagonally shaped with edge angles of 120° , which is an expected kind of behavior, since it has been already observed in the first layer of C_{60} on highly oriented pyrolytic graphite.²¹ The profile analysis of the islands gives an apparent height of $8.8(\pm 0.3) \text{ Å}$ and interestingly does not show medium-scale corrugation that could be expected due to the underlying 6×6 superperiodicity (resulting in a quasi- 6×6 corrugation of the SLG in the STM topography⁹). These findings are consistent with the recent observation made by Cho *et al.*¹⁴

The detail in the inset of Fig. 1(a) shows submolecular resolution, which suggests the adsorbed molecules on SLG are all equally oriented. The submolecular structure of each C_{60} consists of two bright lobes that shall correspond to their MO, which may be considered as a fingerprint for their orientation.^{11,22,23} The most intense features are usually assigned to the C_{60} pentagons. However, in our case, the MO contrasts are slightly varying between subsequent STM images while maintaining the overall character—see Fig. 2. That evidences changes of the probe itself and prevents us from

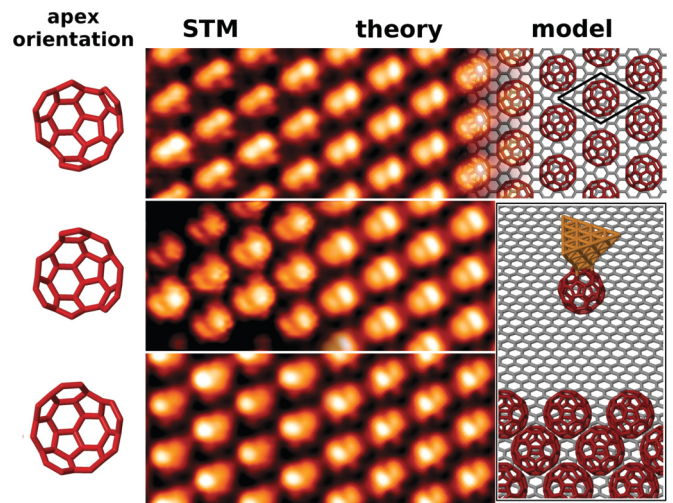


FIG. 2. (Color online) STM topography obtained at 600 mV bias voltage on the 4×4 C_{60} on SLG with varying contrast. The experimental images are compared to the uniquely matching theoretical simulation of STM topography using a C_{60} adsorbed on a metallic tip apex in various orientations, scanned above the model structure of 4×4 C_{60} on SLG. The lower halves of the probe C_{60} are schematically shown near to the appropriate images. The 3D scheme in the inset illustrates the situation.

directly relating the observed contrast to any expected MO of C_{60} molecules previously reported.^{11,22,23} To unambiguously determine the correct orientation of the molecules on the surface based on these data, we have to assume a C_{60} being picked up by the reactive metallic tip apex before the acquisition of the images, since this process is commonplace, especially in LT STM sessions—e.g. Refs. 24 and 25. Therefore, the observed STM contrast on the MO is most likely influenced by imaging of a C_{60} by another C_{60} adsorbed on the tip apex.

Consequently, the most important questions that arise from the experiment are about (i) the detailed role of the vdW in the well-ordered 4×4 C_{60} /SLG system and (ii) the orientation of the C_{60} with respect to the SLG lattice.

We performed extensive DFT-vdW calculations in order to understand the role of the vdW in stabilizing this structure. Several groups have developed DFT-based calculations including the vdW interaction.^{15,26–29} Here we use the LCAO- S^2 previously applied to SLG and graphene-like materials.^{15,16} In this formalism, we consider two contributions. The first arises from the small overlaps between the electronic wave functions of the C_{60} and the SLG, leading to an electronic repulsion, and the second, which is the vdW interaction itself, is due to oscillating dipoles in both interacting systems. These two contributions are treated in perturbation theory from a DFT calculation using the FIREBALL code.^{17,30–32} This method takes into account particularly the π - π interactions since the corresponding overlaps are the dominant effect in this weakly interacting system. The underlying SiC buffer^{33–37} layer was neglected, since the expected energy contribution to the C_{60} total energy due to the vdW interaction is at least an order of magnitude lower than the contribution due to the presence of SLG,¹⁸ considering the large separation of SLG and the buffer layer.³⁸

In the calculations we used more than 20 different adsorption geometries of C_{60} /SLG in a 4×4 periodicity.¹⁸

TABLE I. Total energy values per C_{60} for their various orientations in a 4×4 SLG supercell, with and without considering vdW interactions (E_{vdW} and E_{DFT}) and the associated equilibrium distances d_{vdW} and d_{DFT} . E_{vdW} is a sum of two contributions: the cohesion energy between the C_{60} molecules, $E_{C_{60}-C_{60}}$, and the interaction energy between a C_{60} and the SLG substrate, $E_{C_{60}-\text{SLG}}$. The structure with the lowest energy value is taken as a reference for calculation of the relative total energy ΔE_{vdW} .

C_{60} orientation SLG adsorption site	6:6/30° Hollow	6:6/0° Hollow	Hex/0° Adatom	Hex/0° Dimer
d_{DFT} (Å)	3.4	3.3	3.5	3.6
E_{DFT} (eV)	-0.006	-0.006	-0.004	-0.004
d_{vdW} (Å)	2.7	2.7	2.9	2.9
$E_{C_{60}-C_{60}}$ (eV)	-0.880	-0.871	-0.680	-0.645
$E_{C_{60}-\text{SLG}}$ (eV)	-1.007	-1.010	-1.019	-1.016
E_{vdW} (eV)	-1.887	-1.881	-1.696	-1.659
ΔE_{vdW} (eV)	0.000	+0.006	+0.189	+0.226

These calculations have confirmed that the energetically most favorable structures are indeed those with a high symmetry. To discriminate the contribution of the vdW forces in the global structure, we made DFT calculations with and without incorporation of the vdW forces. The most stable structures among all the probed adsorption sites and molecular orientations are presented in Table I. The molecular orientations are labeled by a C_{60} feature exposed to the surface and the angle of rotation around the z axis (perpendicular to the surface plane) with respect to the diagonal of a 1×1 unit cell of SLG. Thus, the 6:6/0° orientation corresponds to an adsorption of a C_{60} by a dimer shared between two adjacent hexagons parallel to a C-C bond in SLG; the 6:6/30° is identical to the 6:6/0° rotated by 30° around the z axis; hex/0° is a hexagon aligned with the SLG hexagons, etc.¹⁸ There are three possible adsorption sites of high symmetry on the SLG: on top of a C atom (adatom), in the center of a hexagon (hollow), and above the center of a C-C bond (dimer).

In Table I we see that the lowest total energy (E_{vdW}) structure calculated including the vdW interaction is the 6:6/30° in a hollow site of SLG, which is used as the reference value for the relative energy of adsorption (ΔE_{vdW}). The closest structure in terms of energy is the 6:6/0°, also in a hollow site, with a total energy higher by 6.44 meV/ C_{60} . Taking into account that the experiments were performed at 40 K, the thermal energy is about 3 meV, which is approximately half of the difference between the two most favorable structures. Consequently, the system at 40 K should prefer the hollow 6:6/30° adsorption geometry over the hollow 6:6/0°. The rest of the structures present values of the total energy that are much larger, indicating the strong influence of the C_{60} orientation with respect to each other in the value on the vdW interaction. Remarkably, the main difference in the total energy comes from the molecule-molecule interactions ($E_{C_{60}-C_{60}}$) rather than from the interaction with the surface ($E_{C_{60}-\text{SLG}}$), which is only slightly modified when the molecule is placed with a different orientation. As the $E_{C_{60}-C_{60}}$ differs for each adsorption orientation, it has the ultimate role in the final value of the E_{vdW} . Charge transfer from the surface to a C_{60} is negligible, amounting to ≈ 0.03 electrons/ C_{60} , which has been suggested recently.¹⁴

Interestingly, when we perform the total energy calculations without the vdW interactions (E_{DFT}), all four structures result about the same energy (with differences less than 3 meV/ C_{60}) and therefore the orientation of the molecules in the islands on the surface would not have any particular preference under our experimental conditions. The introduction of the vdW interaction results in a considerable reduction of the C_{60} -SLG distance (d_{vdW} compared to d_{DFT}). That is a clear indication that the vdW interactions cannot be neglected in any similar system.

Aware that the total energy difference between 6:6/30° and 6:6/0° is very small, we performed STM simulations for these adsorption geometries to elucidate which is the structure observed experimentally.³⁹ A set of 60 tips consisting of a pyramid of 35 metal atoms and a C_{60} molecule attached to the apex in various geometries has been used⁴⁰ as a probe over both candidates. The calculated images were carefully compared to the experimental images with varying contrast. We found the agreement only for the structures based on the 6:6/30° orientation, as in the example in Fig. 2, where the best agreement is obtained for the 6:6/30° imaged with appropriate orientations of the C_{60} on the tip apex. The couples of bright lobes in the images systematically correspond to a pair of pentagons linked by a dimer between two hexagons, which is crucial to decide the mutual orientation of the molecules in the 4×4 structure. The calculated images are all similar to an image produced by a simple metallic tip, somewhat modified by the effect of the MO of a rotated C_{60} on the tip. Considering the high probability of having a C_{60} on the tip apex leads us to inevitably conclude that any spectroscopic information obtained by scanning tunneling spectroscopy on this system can be significantly distorted. In particular, the width of the gap between the highest occupied and lowest unoccupied states of a C_{60} is likely to be overestimated.¹⁴

So far, we have pointed out the dominance of vdW intermolecular attraction between the C_{60} molecules on SLG. Due to a distinct decay and strength of this force one can expect a qualitatively different dynamical behavior of the molecules in this system. Movement of a single molecule away from the islands is highly unfavorable, because it has to overcome the energy barrier created by the vdW interactions with the nearest neighbors, but it will likely occur along the edge of an island. We observed such a process and it was enhanced by interactions with the scanning tip.¹⁸ We successfully attempted to observe C_{60} diffusion in an experiment by means of fast and reiterate scanning of the same region. Surprisingly, the islands that were not pinned by any defects (step edge, impurity, etc.) revealed a much faster mode of mass transport. Figure 3 shows a sequence of tip-induced changes undergone by an island consisting of 50 C_{60} molecules.

The observed area contains two pinned and thus rather stable islands A and C, plus a free and a very mobile island B which is apparently directed by the sense of the scanning, i.e., alternating upwards and downwards. Importantly, the shape of A and C does not vary strongly from one image to the next. That means the C_{60} migration along the island edges is slow and not many events are missed. A consequent interpretation of the movement of B is only possible by collective motion, as seen in the images between the time stamps 2:48 and 8:24, where both the shape of the island and the number of its molecules remain preserved. Island A serves only as a pivot

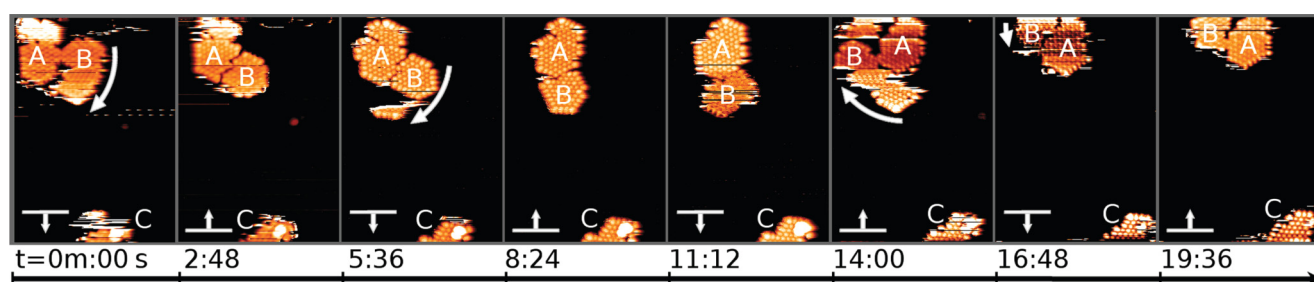


FIG. 3. (Color online) Sequence of STM topographic images taken at 1500 mV and 100 pA on SLG with three islands of C_{60} . Islands A and C are pinned by a step edge and a surface defect, respectively. The whole island B is undergoing movements (marked by curved arrows) that apparently conserve the overall shape of the island between 2:48 and 8:24. The movements of the island are apparently correlated with the direction of scanning (denoted by vertical arrows with horizontal bars).

point as B is changing its orientation with the substrate by 30° . By such rotation of the island, the unit cell is temporarily changed to $(\sqrt{3} \times \sqrt{3})R30^\circ C_{60}$ coincident with a 7×7 SLG, where the density of the molecules in the layer is changed only by 2% (one molecule per 4×4 to three molecules per 7×7). This observation is fully consistent with the balance between the adsorption and cohesion energies predicted by the theory. A diffusion barrier of a C_{60} /SLG is inherently very low and the attractive force between the C_{60} caused by the vdW interactions can reach over distances of several SLG unit cells. Consequently, in the absence of a strong site-specific bonding mechanism, the cohesion force between C_{60} molecules is the crucial factor in the stability of the islands.

In conclusion, the C_{60} /SLG behaves as a prototype of a decoupled adsorbate system governed by vdW forces. Advanced formalism, including vdW forces, is necessary for a

successful determination of the correct adsorption geometry of the molecules. Our results show that the orientation of the molecule within the structure plays a major role in the total energy evaluation. The collective movement of small molecular islands demonstrates the dominant role of the vdW interactions in this system and the decoupling of the C_{60} from the substrate. The agreement of the experimental observation with the total energy and STM image calculations indicates the need for including vdW to account for the weak interactions in sp^2 compounds.

P.M. acknowledges financial support from a Rafael Calvo Rodés scholarship. M.S. and P.J. acknowledge Grant No. GAAV IAA100100905 GACR, Project No. 204/10/0952. C.G. acknowledges the Jose Castillejo Grant from the Spanish Education Ministry and the CSIC JAE-DOC position.

*Corresponding author: svec@fzu.cz

- ¹C. Stadler, S. Hansen, I. Kröger, C. Kumpf, and E. Umbach, *Nat. Phys.* **5**, 153 (2009).
- ²P. N. Dickerson, A. M. Hibberd, N. Oncel, and S. L. Bernasek, *Langmuir* **26**, 18155 (2010).
- ³F. Hanke, S. Haq, R. Raval, and M. Persson, *ACS Nano* **5**, 9093 (2011).
- ⁴A. Tkatchenko, L. Romaner, O. T. Hofmann, E. Zojer, C. Ambrosch-Draxl, and M. Scheffler, *MRS Bull.* **35**, 435 (2010).
- ⁵V. G. Ruiz, W. Liu, E. Zojer, M. Scheffler, and A. Tkatchenko, *Phys. Rev. Lett.* **108**, 146103 (2012).
- ⁶K. S. Novoselov, A. K. Geim, S. V. Morozov, D. Jiang, Y. Zhang, S. V. Dubonos, I. V. Grigorieva, and A. A. Firsov, *Science* **306**, 666 (2004).
- ⁷H. W. Kroto, J. R. Heath, S. C. O'Brien, R. F. Curl, and R. E. Smalley, *Nature (London)* **318**, 162 (1985).
- ⁸H. Shin, S. E. O'Donnell, P. Reinke, N. Ferralis, A. K. Schmid, H. I. Li, A. D. Novaco, L. W. Bruch, and R. D. Diehl, *Phys. Rev. B* **82**, 235427 (2010).
- ⁹P. Martensson, F. Owman, and L. I. Johansson, *Phys. Status Solidi B* **202**, 501 (1997).
- ¹⁰H. Huang, W. Chei, S. Chen, and A. T. S. Wee, *ACS Nano* **12**, 2513 (2008).
- ¹¹P. J. Moriarty, *Surf. Sci. Rep.* **65**, 175 (2010).
- ¹²J. Lu, P. S. E. Yeo, Y. Zheng, Z. Yang, Q. Bao, C. K. Gan, and K. P. Loh, *ACS Nano* **6**, 944 (2012).

- ¹³G. Li, H. T. Zhou, L. D. Pan, Y. Zhang, and J. H. Mao, *Appl. Phys. Lett.* **100**, 013304 (2012).
- ¹⁴J. Cho, J. Smerdon, L. Gao, O. Süzer, J. R. Guest, and N. P. Guisinger, *Nano Lett.* **12**, 3018 (2012).
- ¹⁵Y. J. Dappe, J. Ortega, and F. Flores, *Phys. Rev. B* **79**, 165409 (2009).
- ¹⁶Y. J. Dappe, M. A. Basanta, F. Flores, and J. Ortega, *Phys. Rev. B* **74**, 205434 (2006).
- ¹⁷J. P. Lewis, P. Jelínek, J. Ortega, A. A. Demkov, D. G. Trabada, B. Haycock, H. Wang, G. Adams, J. K. Tomfohr, E. Abad, H. Wang, and D. A. Drabold, *Phys. Status Solidi B* **248**, 1989 (2011).
- ¹⁸See Supplemental Material at <http://link.aps.org/supplemental/10.1103/PhysRevB.86.121407> for more information.
- ¹⁹W. Chen, H. L. Zhang, H. Xu, E. S. Tok, K. P. Loh, and A. T. S. Wee, *J. Phys. Chem. B* **110**, 21873 (2006).
- ²⁰W. Chen, S. Chen, H. L. Zhang, H. Xu, D. C. Qi, X. Y. Gao, K. P. Loh, and A. T. S. Wee, *Surf. Sci.* **610**, 2994 (2007).
- ²¹H. Liu and P. Reinke, *J. Chem. Phys.* **124**, 164707 (2006).
- ²²X. Lu, M. Grobis, K. H. Khoo, S. G. Louie, and M. F. Crommie, *Phys. Rev. B* **70**, 115418 (2004).
- ²³G. Schull and R. Berndt, *Phys. Rev. Lett.* **99**, 226105 (2007).
- ²⁴G. Schull, T. Frederiksen, M. Brandbyge, and R. Berndt, *Phys. Rev. Lett.* **103**, 206803 (2009).
- ²⁵B. W. Heinrich, M. V. Rastei, D.-J. Choi, T. Frederiksen, and L. Limot, *Phys. Rev. Lett.* **107**, 246801 (2011).

- ²⁶D. C. Langreth, M. Dion, H. Rydberg, E. Schröder, P. Hyldgaard, and B. I. Lundqvist, *Int. J. Quantum Chem.* **101**, 599 (2005).
- ²⁷A. Tkatchenko and M. Scheffler, *Phys. Rev. Lett.* **102**, 073005 (2009).
- ²⁸S. Lebegue, J. Harl, T. Gould, J. G. Angyan, G. Kresse, and J. F. Dobson, *Phys. Rev. Lett.* **105**, 196401 (2010).
- ²⁹G.-X. Zhang, A. Tkatchenko, J. Paier, H. Appel, and M. Scheffler, *Phys. Rev. Lett.* **107**, 245501 (2011).
- ³⁰J. P. Lewis, K. R. Glaesemann, G. A. Voth, J. Fritsch, A. A. Demkov, J. Ortega, and O. F. Sankey, *Phys. Rev. B* **64**, 195103 (2001).
- ³¹P. Jelinek, H. Wang, J. P. Lewis, O. F. Sankey, and J. Ortega, *Phys. Rev. B* **71**, 235101 (2005).
- ³²M. A. Basanta, Y. J. Dappe, P. Jelinek, and J. Ortega, *Comput. Mater. Sci.* **39**, 759 (2007).
- ³³J. Hass, W. A. de Heer, and E. H. Conrad, *J. Phys.: Condens. Matter* **20**, 323202 (2008).
- ³⁴S. Kim, J. Ihm, H. J. Choi, and Y.-W. Son, *Phys. Rev. Lett.* **100**, 176802 (2008).
- ³⁵C. Riedl, C. Coletti, T. Iwasaki, A. A. Zakharov, and U. Starke, *Phys. Rev. Lett.* **103**, 246804 (2009).
- ³⁶J. Ristein, S. Mammadov, and T. Seyller, *Phys. Rev. Lett.* **108**, 246104 (2012).
- ³⁷C. Xia, S. Watcharinyanon, A. A. Zakharov, R. Yakimova, L. Hultman, L. I. Johansson, and C. Virojanadara, *Phys. Rev. B* **85**, 045418 (2012).
- ³⁸F. Varchon, R. Feng, J. Hass, X. Li, B. N. Nguyen, C. Naud, P. Mallet, J.-Y. Veuillen, C. Berger, E. H. Conrad, and L. Magaud, *Phys. Rev. Lett.* **99**, 126805 (2007).
- ³⁹J. M. Blanco, F. Flores, and R. Perez, *Prog. Surf. Sci.* **81**, 403 (2006).
- ⁴⁰G. Schull, Y. J. Dappe, C. Gonzalez, H. Bolou, and R. Berndt, *Nano Lett.* **11**, 3142 (2011).